Phys Chem Minerals (2006) 33: 1–9
DOI 10.1007/s00269-005-0008-3

ORIGINAL PAPER

Ichiro Ohno · Kazumi Harada · Chihiro Yoshitomi

Temperature variation of elastic constants of quartz across the α - β transition

Received: 14 April 2004 / Accepted: 4 April 2005 / Published online: 3 January 2006

Abstract The $\alpha - \beta$ transition of quartz was successfully observed with using a single sample by means of the rectangular parallelepiped resonance (RPR) method. An oriented rectangular parallelepiped of α-quartz single crystal was prepared and the resonant frequencies of 30–11 vibrational modes were measured from room temperature to 700°C. The softening of quartz crystal was observed as the significant reduction of resonant frequencies near the α–β transition. The present study is the first application of the RPR method to the study of phase transition. The complete set of elastic constants of α- and β-quartz were determined as a function of temperature by the least-squares inversion of the measured frequency data obtained by a single run. This is a merit yielded by the RPR method. It is shown near the $\alpha - \beta$ transition in both α- and β-quartz that the elastic parameters decrease proportionally to $|T-T_0|^{-n}$, where T is temperature and T_0 is the transition temperature, 573.0°C for α-quartz and 574.3°C for β-quartz. It was also seen that linear incompressibilities $K_1 = (C_{11} + C_{12} + C_{13})/3$ and $K_3 = (C_{33} + 2C_{13})/3$ decrease rapidly toward the transition, whereas, shear moduli C_{44}, $C_{S1} = (C_{11} + C_{33} - 2C_{13})/4$ and $C_{S3} = (C_{11} - C_{12})/2 = C_{66}$ decrease only slightly. The shear modulus $C_{S3} = C_{66}$ increased slightly in α-quartz. The elastic properties of isotropic aggregate of quartz were calculated, and it is shown that the longitudinal wave velocity significantly decreases at the $\alpha - \beta$ transition, whereas, the shear wave velocity decreases only slightly.

I. Ohno (✉) · K. Harada · C. Yoshitomi
Department of Earth Sciences, Ehime University,
2-5 Bunkyou-cho, Matsuyama, 790-8577 Japan
E-mail: ohno@sci.ehime-u.ac.jp
Tel.: +81-89-9279647
Fax: +81-89-9279630

Introduction

It is well known that trigonal α-quartz transforms to an intermediate incommensurate phase at $T_0 = 573.0$°C, and then to hexagonal β-quartz at $T_1 = 574.3$°C. The elasticity of α-quartz has been studied by many authors (e.g., Atanasoff and Hart 1941; Koga et al. 1958; Bechmann 1958; McSkimin et al. 1965; Scott 1972; Ohno 1994). The data regarding β-quartz have been reported by Kammer et al. (1948), and Zubov and Firsova (1962). The temperature range measured by Kammer et al. (1948) is limited within the β-quartz region, from 580°C to 800°C. Measurement across the $\alpha - \beta$ transition is only the report by Zubov and Firsova (1962), and the behavior of quartz near the α–β transition remains of interest to researchers.

Ohno (1994) measured the elasticity of α-quartz as a function of temperature by means of the rectangular parallelepiped resonance (RPR) method (Ohno 1976; Ohno et al. 1986). Although that measurement by Ohno (1994) was limited to the α-quartz region, it suggested the possibility of monitoring the α–β transition using a single sample by means of the RPR method. The RPR method is excellent to investigate the temperature variation of the elasticity of lower symmetry crystals such as trigonal, because we can acquire the frequency data of a redundant number of modes at once to determine all of the independent elastic constants simultaneously without repeating runs. The purpose of this study is to extend the RPR measurement across the $\alpha - \beta$ transition. This is the first application of the RPR method to phase transition.

α-Quartz is a piezoelectric material. In principle, the effect of piezoelectricity should be taken into account for the determination of elastic constants. However, Ohno (1990) studied the effect of piezoelectricity on the eigenfrequencies measured by the RPR method, and demonstrated that the difference in the determined elastic constants is 0.5% at most, whether or not, piezoelectricity is taken into account. Therefore, for simplicity, piezoelectricity is neglected in the present study.

Experimental details

An oriented rectangular parallelepiped specimen was prepared from a synthetic quartz crystal. The edge lengths were 1.622 ± 0.001 mm (parallel to *a*-axis), 2.915 ± 0.001 mm, and 3.193 ± 0.001 mm (parallel to *c*-axis). The density was 2.641 g/cm^3 from the mass and the volume. This bulk density is 0.3% smaller than the X-ray density of α-quartz, 2.65 g/cm^3.

A buffer rod system (Goto and Anderson 1988, 1989) was adopted for high temperature RPR measurement. The specimen was held between a pair of thin, long buffer rods made of alumina ceramics. A lead titanate–zirconate transducer was attached at the other end of each buffer rod functioning as a transmitter or a receiver. The specimen and the upper portion of the buffer rods were placed in an electric furnace, while the transducers were kept out of the furnace. One of the buffer rods was set on a balance in order to keep the force holding the specimen constant during the high temperature measurements.

The temperature of the sample was measured by means of a chromel–alumel thermocouple. The hot joint of the thermocouple was located at a radial distance of about 0.5 mm from the sample surface. The electric furnace was 35 mm in inner diameter, and 100 mm in length. The radial temperature gradient at the sample position was measured to be 0.5°C/mm at 500°C. From the temperature gradient and the sample size, the accuracy of the temperature measurement was estimated to be ±1°C near 500°C.

A continuous sinusoidal voltage was input to one of the transducers (CW method), and the output was monitored with an oscilloscope and rectified to draw a spectrum with an X–Y recorder. By scanning the frequency of the input voltage, the resonance spectrum was obtained. The frequency of resonance peaks was measured to the digit of 100 Hz. The measurement was repeated in increments of several tens of degrees from room temperature up to 487.5°C, and in increments of several single-digit degrees up to 571°C. After the measurement at 571°C, the temperature was increased to 696°C across the transition point. Then, similar measurements were repeated from 696°C to 575.5°C. The temperature fluctuation was within ±0.5°C during the measurement at each temperature.

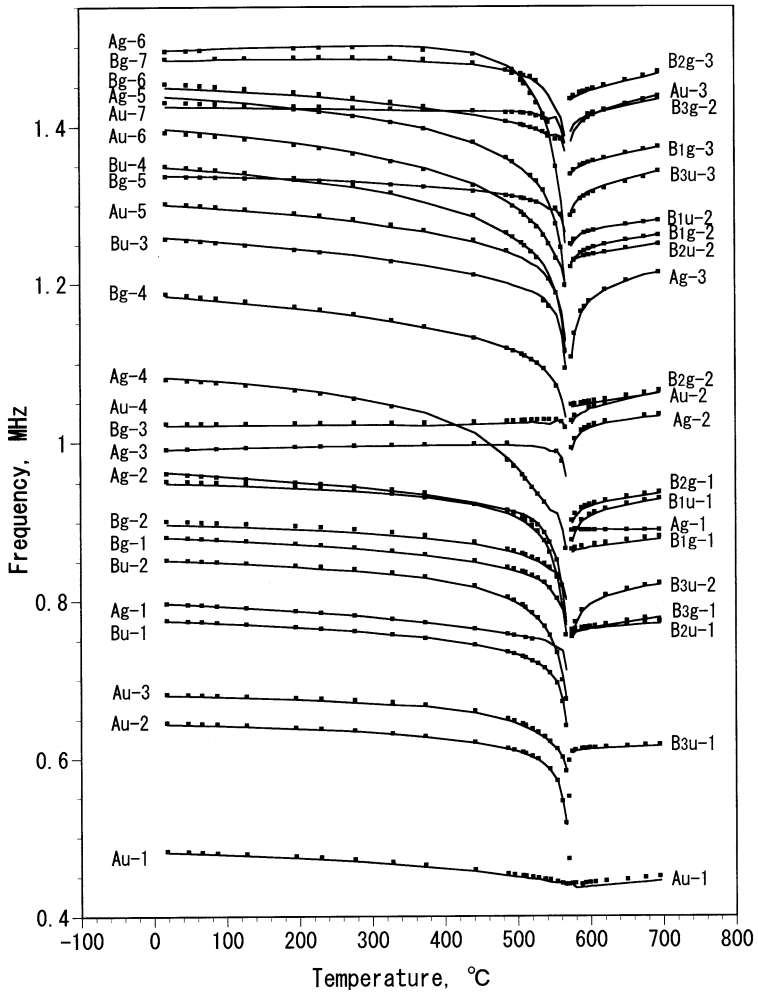

Fig. 1 Measured and calculated frequencies plotted as a function of temperature; *squares* measured frequencies; *solid lines* theoretical frequencies calculated for the determined elastic constants given in Table 2

No direct examination was performed in order to check whether the specimen was a single crystal of β-quartz at temperatures above the transition point. However, in the case of the present specimen, transformation to a single crystal of β-quartz with a common c-axis was likely. In fact, the observed 21 peaks were consistently assigned to theoretical frequencies calculated on the assumption that the specimen was an oriented rectangular parallelepiped of a hexagonal crystal, as will be addressed later.

Data reduction

The small squares in Fig. 1 represent the observed frequencies plotted as a function of temperature. The first 30 peaks between 0.4 MHz to 1.6 MHz were measured from room temperature to 538°C. The number of peaks decreased toward the $\alpha-\beta$ transition, but several peaks were still observed at 571°C. After the transition, a total of 21 peaks were measured. The frequency of most modes decreased toward the α–β transition from both sides. However, in a few of the modes, the frequency increases slightly up to 540°C, and then drops down toward the transition, as seen in B_g-3 and A_u-4 in α-quartz. The mode A_g-1 in β-quartz shows similar behavior.

Figure 2 shows an example of the temperature variation of the spectrum measured around the first mode A_u-1. As the temperature increased from room temperature, the peak shifted to a lower frequency up to 571°C. At higher temperatures than the transition point, the peak recovered again to a high frequency. The frequency of A_u-1 mode varied almost continuously across the transition, while all other modes were discontinuously, as shown in Fig. 1.

The first 30 peaks measured at temperatures below 538°C were readily assigned to the theoretical frequencies calculated for the elastic constants by Ohno (1994). Between 545°C and 571°C, mode identification became difficult due to an increasingly rapid decrease in the frequency within a narrow temperature change and also because of a crossover of frequencies between modes. However, 17–11 modes were identified at temperatures

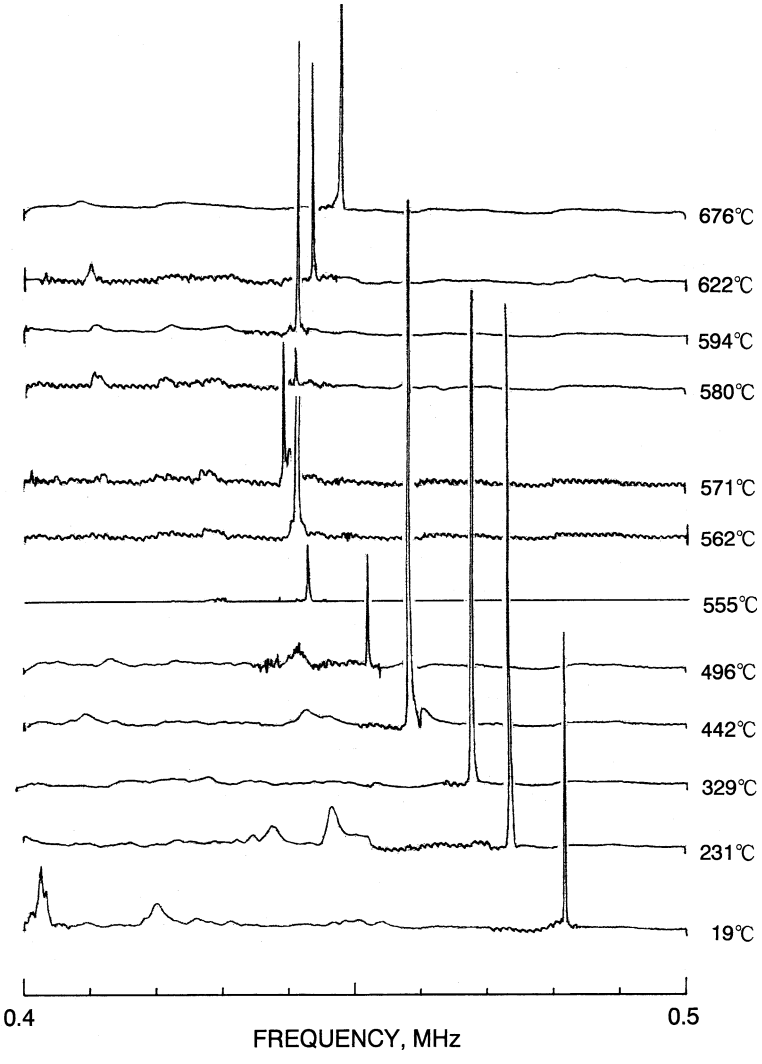

Fig. 2 Observed spectra recorded at various temperatures showing the temperature-induced shift of the lowest mode, A_u-1

between 545°C and 567°C, and the elastic constants could thus be determined. At 571°C, four peaks were observed. They were plotted in Fig. 1, but do not correspond to any theoretical curve because the elastic constants could not determined with four peaks. In the β-quartz region, the first 21 peaks were measured and identified consistently based on the hexagonal elastic constants determined by Zubov and Firsova (1962).

The elastic constants were determined by the linearized least-squares inversion of the measured frequencies at each temperature. The method by Oda et al. (1993) was effectively used in the inversion, which gives the partial derivatives of frequency with respect to the elastic constant, $\partial f/\partial C_{ij}$. At high temperatures, the edge lengths of the specimen were calculated based on the thermal expansion data provided by Ackerman and Sorrell (1974). The solid lines in Fig.1 show the theoretical frequencies calculated for the determined elastic constants

Results

The determined elastic constants are listed in Table 1, and are plotted as a function of temperature in Fig.3. Near the transition temperature, the elastic constants varied very rapidly. According to Scott (1972), the rapid temperature variation of physical property X near the second order phase transition is represented by $X \propto |T_0 - T|^{-n}$, where exponent n is constant. Based on this expression, the elastic parameters for the α-quartz region were plotted versus the temperature difference from the transition, $T_0 - T$, in logarithmic scale in Fig. 4, where $T_0 = 573.0$°C. Similarly, the elastic parameters for the β-quartz region were plotted versus $T - T_1$ in Fig. 5, where $T_1 = 574.3$°C, the transition temperature from the incommensurate phase to β-quartz.

Table 1 Elastic constants of α- and β-quartz in GPa. The linear combinations of elastic constants, K_1, K_3, C_{S1}, and $C_{66} = C_{S3}$, are also given: $K_1 = (C_{11} + C_{12} + C_{13})/3$, $K_3 = (C_{33} + 2C_{13})/3$, $C_{S1} = (C_{11} + C_{33} - 2C_{13})/4$, and $C_{66} = (C_{11} - C_{12})/2 = C_{S3}$

Temperature (°C)	C_{11} (GPa)	C_{33} (GPa)	C_{44} (GPa)	C_{12} (GPa)	C_{13} (GPa)	C_{14} (GPa)	K_1 (GPa)	K_3 (GPa)	C_{S1} (GPa)	C_{66} (GPa)
19	88.2 ±0.3	107.2 ±0.8	58.5 ±0.4	6.5 ±0.7	12.4 ±0.6	18.8 ±0.4	35.7	44.0	42.7	40.9
48	88.1	106.7	58.1	6.0	12.2	18.7	35.4	43.7	42.6	41.0
67	87.9	106.3	57.8	5.6	12.1	18.7	35.2	43.5	42.5	41.2
88	87.9	105.6	57.6	4.9	11.8	18.9	34.9	43.1	42.5	41.5
128.5	87.7	104.6	57.0	4.0	11.4	19.0	34.4	42.5	42.4	41.9
196	87.0	103.0	56.1	1.9	10.8	19.1	33.2	41.5	42.1	42.5
231	86.7	102.0	55.5	0.8	10.2	19.2	32.5	40.8	42.1	43.0
277	86.1 ±0.2	100.5 ±0.6	54.6 ±0.4	−0.6 ±0.5	9.3 ±0.4	19.1 ±0.3	31.6	39.7	42.0	43.4
329	85.6	98.5	53.4	−2.6	8.2	19.1	30.4	38.3	41.9	44.1
374	84.7	97.5	51.8	−4.1	8.1	18.5	29.6	37.9	41.5	44.4
442	82.9	93.7	49.9	−8.8	5.6	18.4	26.6	35.0	41.3	45.8
487.5	80.6 ±0.2	90.5 ±0.4	47.3 ±0.3	−12.8 ±0.4	3.4 ±0.3	17.2 ±0.3	23.8	32.4	41.1	46.7
496	80.2	89.7	46.8	−13.9	2.8	17.0	23.1	31.8	41.1	47.1
508	79.3	88.5	46.2	−15.1	1.9	16.7	22.0	30.8	41.0	47.2
512	78.9	87.8	45.7	−15.5	1.3	16.3	21.6	30.1	41.0	47.2
521	78.1	86.6	45.0	−16.8	−0.2	15.8	20.3	28.7	41.3	47.4
529	77.0 ±0.3	85.4 ±0.3	44.6 ±0.3	−17.4 ±0.5	−0.6 ±0.4	15.4 ±0.4	19.5	27.8	41.2	47.2
538	75.7	84.0	43.4	−18.6	−2.1	14.4	18.4	26.6	40.9	47.2
545	74.6 ±0.6	82.4 ±0.7	42.8 ±0.6	−20.4 ±0.8	−2.8 ±0.6	14.1 ±0.8	17.1	25.6	40.6	47.5
555	73.1	81.2	42.0	−24.6	−5.0	13.5	14.5	23.7	41.1	48.9
562	70.6	74.2	40.6	−25.7	−6.6	11.0	12.8	20.3	39.5	48.1
567	69.2	67.4	39.6	−28.7	−7.3	10.7	11.1	17.6	37.8	48.9
[$\alpha-\beta$ transition]										
575.5	102.4 ±0.5	100.2 ±1.0	35.7 ±0.1	0.9 ±1.3	20.3 ±0.8	–	41.2	47.0	40.5	50.8
580	108.2	105.5	35.8	7.0	25.8	–	47.0	52.3	40.5	50.6
589	115.2	109.2	36.0	14.1	30.9	–	53.4	57.0	40.6	50.5
594	116.8	110.4	36.0	15.5	32.3	–	54.9	58.3	40.6	50.7
600	119.1	112.9	36.2	17.8	34.8	–	57.2	60.8	40.6	50.6
607	120.7	113.2	36.2	19.2	35.6	–	58.5	61.5	40.7	50.8
622	123.9 ±0.9	115.4 ±1.1	36.4 ±0.1	22.0 ±1.3	38.2 ±0.9	–	61.4	63.9	40.7	50.9
651	127.3	118.0	36.8	24.8	41.2	–	64.4	66.8	40.7	51.2
676	130.2	120.3	37.1	27.4	43.7	–	67.1	69.2	40.8	51.4
696	131.1 ±1.1	120.5 ±1.2	37.4 ±0.1	27.8 ±1.5	44.0 ±1.1	–	67.6	69.5	40.9	51.7

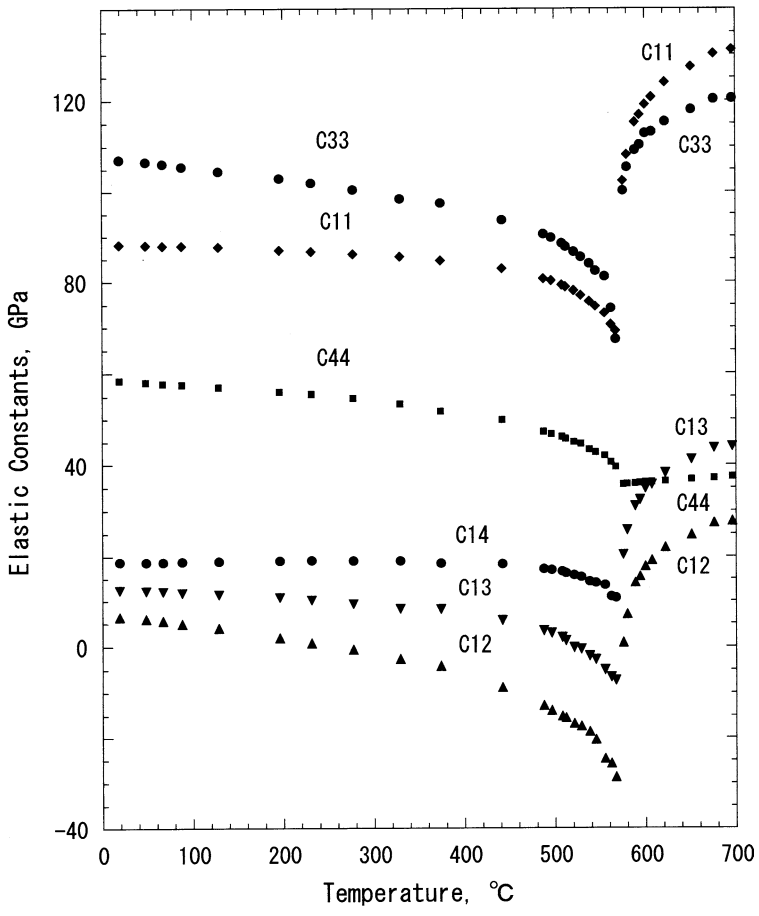

Fig. 3 Temperature variation of elastic constants determined in this study. *Diamonds* C_{11}; *circles* C_{33} and C_{14}; *squares* C_{44}; and *triangles* C_{12} and C_{13}

In Figs. 4 and 5, the linear combinations of C_{ij}, K_1, K_3, C_{S1}, and $C_{S3} = C_{66}$ were used instead of the elastic constants C_{11}, C_{33}, C_{12}, and C_{13}. Here, $K_1 = (C_{11} + C_{12} + C_{13})/3$ and $K_3 = (C_{33} + 2C_{13})/3$ are linear incompressibilities for isotropic dilatation in directions perpendicular and parallel to c-axis, respectively. $C_{S1} = (C_{11} + C_{33} - 2C_{13})/4$ and $C_{S3} = (C_{11} - C_{12})/2 = C_{66}$ are shear moduli to relate the directions perpendicular or parallel to c-axis. The exponent n for these elastic parameters were determined from the data given in Figs.4 and 5; the exponents are listed in Table 2. Figure 4 and Table 2 show clearly that the linear incompressibilities K_1 and K_3 and the trigonal constant C_{14} decreased rapidly toward the transition, whereas the shear moduli C_{44} and C_{S1} decreased only slightly; $C_{S3} = C_{66}$ was shown to slightly increase. This situation in α-quartz is clearer in β-quartz, as shown in Fig. 5, where the shear moduli C_{44}, C_{S1}, and $C_{S3} = C_{66}$ revealed horizontal lines, whereas, K_1 and K_3 decreased with a steep slope.

The trigonal constant C_{14} is to vanish in β-quartz due to the hexagonal symmetry. However, the temperature variation of C_{14}, shown in Fig. 3, suggests that C_{14} still possessed a small finite value at the transition point. From the extrapolation of the line shown in Fig. 4, C_{14} is 5 GPa at T-$T_0 = 0.1°$.

Discussion

In the determination of elastic constants of α-quartz, the number of modes taken into the inversion changed from 30 at low temperature to 11 at 567°C. This reduction of mode number at high temperature might influence the determined elastic constants. In order to examine this point, inversion with using 11 modes was done at several temperatures. The used 11 modes were selected as same as at 567°C as possible, because the same modes were not always observed at every temperature. The result is listed in Table 3. When Table 3 is compared with Table 1, the differences in elastic constants are almost in

Table 2 The values of the exponent n in the following relation: elastic parameter $\propto (T_0 - T)^{-n}$ for α-quartz, and $(T-T_1)^{-n}$ for β-quartz, where T is temperature, $T_0 = 573.0$°C, and $T_1 = 574.3$°C

Elastic parameter	α-quartz	β-quartz
K_1	0.296	0.110
K_3	0.226	0.086
C_{14}	0.191	–
C_{44}	0.068	0.0064
C_{S1}	0.028	0.0015
$C_{S3} = C_{66}$	−0.017	0.0017

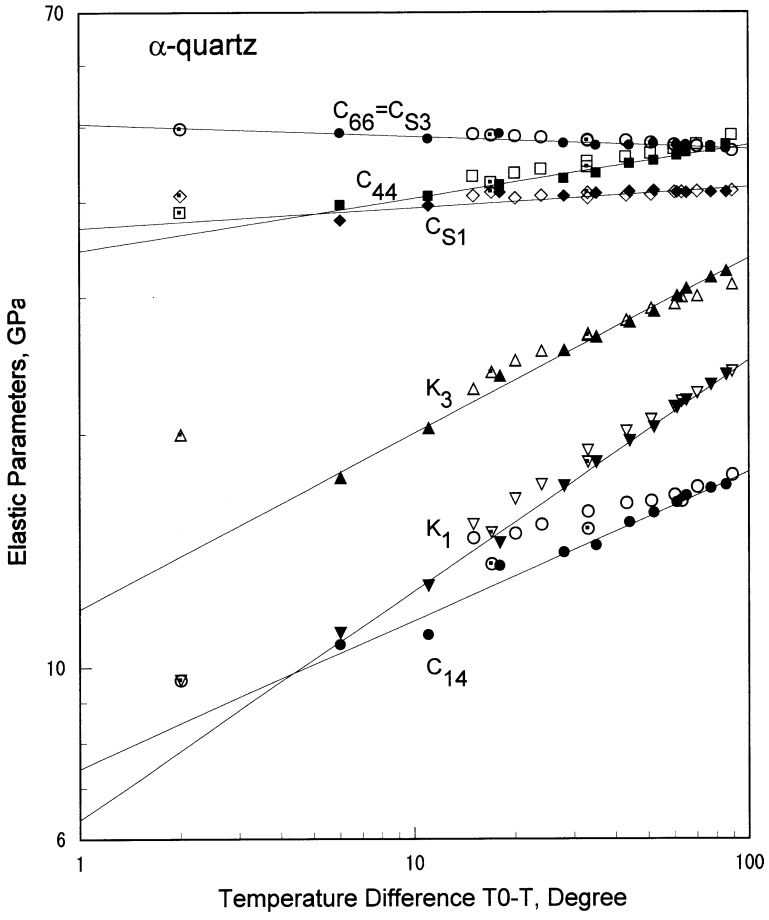

Fig. 4 Elastic parameters of α-quartz near the $\alpha - \beta$ transition. K_1, K_3, C_{44}, C_{S1}, $C_{S3} = C_{66}$, and C_{14} are plotted as a function of temperature difference from the transition temperature, T-T_0, on a logarithmic scale, where $T_0 = 573.0$°C, $K_1 = (C_{11} + C_{12} + C_{13})/3$, $K_3 = (C_{33} + 2C_{13})/3$, $C_{S1} = (C_{11} + C_{33} - 2C_{13})/4$, and $C_{S3} = (C_{11} - C_{12})/2 = C_{66}$. *Triangles* K_1 and K_3; *squares* C_{44}; *diamonds* C_{S1}; *circles* $C_{S3} = C_{66}$ and C_{14}; *solid symbols* results from this study; *open symbols* from Ohno (1994); *dotted symbols* from Zubov and Firsova (1962). *Straight lines* indicate the best fit line to the data of this study

the same order of magnitude as the standard deviation in the least squares determination. Therefore, the change of mode number used in the inversion does not cause any important influence in the determined elastic constants.

On the elastic parameters of β-quartz shown in Fig. 5, shear moduli C_{S1} and $C_{S3} = C_{66}$ determined in this study agree well with those by Kammer et al. (1948) and Zubov and Firsova (1962). The constant C_{44} reported by Kammer et al. (1948) shows slight increase

Table 3 (a) Elastic constants determined by using almost the same 11 modes as used at 567°C; (b) standard deviation; (c) difference from elastic constants given in Table 1

Temperature (°C)		C_{11} (GPa)	C_{33} (GPa)	C_{44} (GPa)	C_{12} (GPa)	C_{13} (GPa)	C_{14} (GPa)	K_1 (GPa)	K_3 (GPa)	C_{S1} (GPa)	C_{66} (GPa)
19	(a)	87.8	107.7	58.7	6.7	12.1	18.3	35.4	44.0	42.8	40.7
	(b)	±0.2	±0.5	±0.3	±0.6	±0.4	±0.3				
	(c)	−0.4	0.5	−0.3	−0.1	−0.3	−0.5	−0.3	0.0	0.1	−0.2
277	(a)	86.6	99.9	54.5	−1.4	8.7	19.3	31.3	39.2	42.2	44.0
	(b)	±0.3	±0.7	±0.4	±0.8	±0.5	±0.4				
	(c)	0.5	−0.6	−0.1	−0.8	−0.6	0.2	−0.3	−0.5	0.2	0.6
487.5	(a)	81.0	90.3	47.2	−13.4	2.8	17.2	23.4	31.9	41.4	47.2
	(b)	±0.3	±0.4	±0.3	±0.6	±0.5	±0.3				
	(c)	0.4	−0.2	−0.1	−0.6	−0.6	0.0	−0.4	−0.5	0.3	0.5
529	(a)	78.1	85.5	45.0	−18.9	0.6	16.0	19.9	28.9	40.6	48.5
	(b)	±0.3	±0.3	±0.2	±0.4	±0.4	±0.2				
	(c)	1.1	0.1	0.4	−1.5	1.2	0.6	0.4	1.1	−0.6	1.3
545	(a)	76.0	83.0	43.1	−23.3	−2.9	15.2	16.6	25.7	41.2	49.7
	(b)	+0.8	+0.7	+0.7	+1.0	+0.5	+1.0				
	(c)	1.4	0.6	0.3	−2.9	−0.1	1.1	−0.5	0.1	0.6	2.2

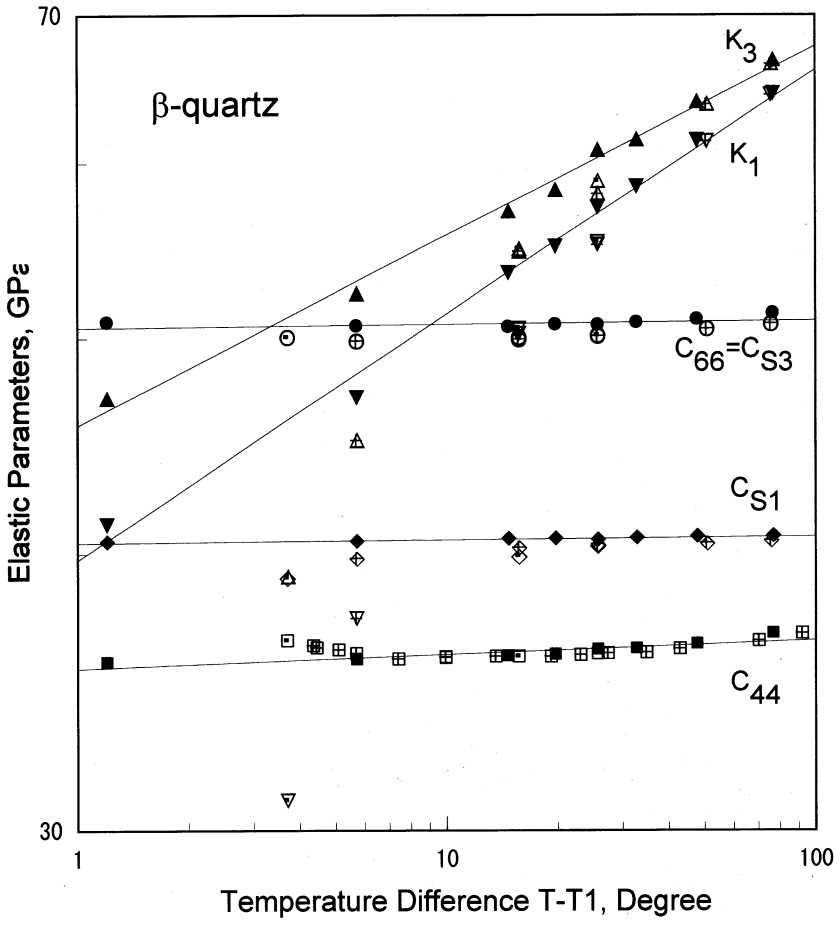

Fig. 5 Elastic parameters of β-quartz near the $\alpha - \beta$ transition, plotted as a function of temperature difference from the transition temperature, T-T_1, on a logarithmic scale, where $T_1 = 574.3$°C. $K_1 = (C_{11} + C_{12} + C_{13})/3$, $K_3 = (C_{33} + 2C_{13})/3$, $C_{S1} = (C_{11} + C_{33} - 2C_{13})/4$, and $C_{S3} = (C_{11} - C_{12})/2 = C_{66}$. *Triangles* K_1 and K_3; *squares* C_{44}; *diamonds* C_{S1}; *circles* $C_{S3} = C_{66}$ and C_{14}; *solid symbols* results from this study; *dotted symbols* from Zubov and Firsova (1962); *crossed symbols* from Kammer et al. (1948). *Straight lines* indicate the best fit line to the data of this study

toward the transition temperature $T_1 = 574.3$°C with a minimum at 580°C, whereas, the present data show decreasing behavior even at 575.5°C. Regarding K_1 and K_3, while the previous data show very rapid decrease toward the transition, the present data show the trend represented by power law.

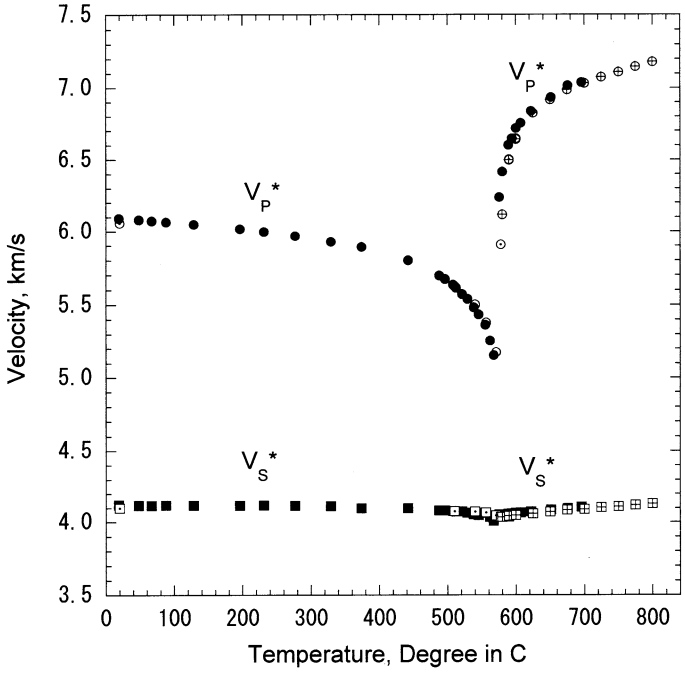

Fig. 6 Temperature variation of longitudinal and shear wave velocities, V_P^* and V_S^*, respectively, Voigt-Reuss-Hill averaged aggregate velocity; *solid symbols* results from this study, *dotted symbols* from Zubov and Firsova (1962); *crossed symbols* from Kammer et al. (1948)

Table 4 Elasticity of Voigt-Reuss-Hill averaged aggregate of α- and β-quartz calculated from Table 1

Temperature (°C)	Density (g/cm^3)	K^*_{VRH} (GPa)	G^*_{VRH} (GPa)	v^*	V^*_P (km/s)	V^*_S (km/s)
19	2.641	38.17	44.86	0.078	6.091	4.121
48	2.639	37.93	44.77	0.076	6.082	4.119
67	2.638	37.69	44.71	0.075	6.074	4.117
88	2.636	37.35	44.73	0.072	6.066	4.119
128.5	2.632	36.81	44.63	0.068	6.050	4.118
196	2.623	35.70	44.46	0.060	6.017	4.117
231	2.618	35.02	44.40	0.054	5.999	4.118
277	2.611	34.06	44.22	0.047	5.969	4.115
329	2.602	32.78	44.02	0.036	5.928	4.113
374	2.595	32.06	43.56	0.032	5.894	4.097
442	2.582	29.07	43.33	0.002	5.800	4.097
487.5	2.571	26.33	42.82	−0.027	5.697	4.081
496	2.569	25.65	42.76	−0.036	5.673	4.080
508	2.566	24.60	42.65	−0.049	5.635	4.077
512	2.565	24.08	42.56	−0.056	5.614	4.073
521	2.562	22.83	42.53	−0.075	5.572	4.074
529	2.560	22.17	42.29	−0.083	5.540	4.064
538	2.557	20.82	42.02	−0.103	5.482	4.054
545	2.555	19.64	41.83	−0.123	5.433	4.047
555	2.550	17.19	42.11	−0.174	5.363	4.064
562	2.544	15.02	41.40	−0.218	5.254	4.034
567	2.536	13.04	40.73	−0.265	5.154	4.008
[α−β transition]						
575.5	2.522	42.97	41.41	0.135	6.239	4.052
580	2.522	48.63	41.42	0.168	6.417	4.052
589	2.523	54.56	41.52	0.196	6.601	4.057
594	2.523	55.98	41.57	0.202	6.646	4.060
600	2.523	58.36	41.64	0.212	6.719	4.063
607	2.523	59.44	41.71	0.216	6.754	4.066
622	2.523	62.18	41.86	0.225	6.839	4.073
651	2.523	65.18	42.12	0.234	6.936	4.086
676	2.523	67.78	42.31	0.242	7.016	4.095
696	2.523	68.24	42.55	0.242	7.038	4.107

K^*_{VRH} and G^*_{VRH} : bulk modulus and rigidity, respectively, according to the Voigt-Reuss-Hill scheme; v^* Poisson's ratio; V^*_{P} and V^*_{S} : longitudinal and shear wave velocity, respectively. Here, an asterisk indicates aggregate properties

Elastic wave velocities may be of more interest than elastic constants from the viewpoint of the behavior of quartz in the earth's crust. The bulk and rigidity moduli of isotropic aggregate, K^*_{VRH} and G^*_{VRH}, and Poisson's ratio v^* were calculated according to the Voigt-Reuss-Hill averaging scheme, and are listed in Table 4. In α-quartz, K^*_{VRH} possesses a smaller value than G^*_{VRH} over the temperature range measured, and Poisson's ratio is very small and even negative at high temperatures. In this sense, α-quartz is an anomalous material, whereas, β-quartz behaves normally. The longitudinal and shear wave velocities in quartz aggregate, V^*_{P} and V^*_{S} respectively, were also calculated and are illustrated in Fig. 6. It was clearly demonstrated that V^*_{P} decreased significantly near the $\alpha - \beta$ transition, whereas V^*_{S} was only slightly influenced by the transition (Fig. 6). V^*_{P} and V^*_{S} obtained in this study are in good agreement with those by Kammer et al. (1948) and Zubov and Firsova (1962).

Acknowledgements The authors thank the reviewers, Drs. D. Isaak, S. Senogeikin and D. Lakshtanov. Their comments were very much helpful to improve the manuscript.

References

Ackermann RJ, Sorrell CA (1974) Thermal expansion and the high-low transformation in quartz. I. High-temperature X-ray studies. J Appl Cryst 7:461–467

Atanasoff JV, Hart PJ (1941) Dynamical determination of the elastic constants and their temperature coefficients for quartz. Phys Rev 59:85–96

Bechmann R (1958) Elastic and piezoelectric constants of alpha-quartz. Phys Rev 110:1060–1061

Goto T, Anderson OL (1988) Apparatus for measuring elastic constants of single crystal by a resonance technique up to 1825 K. Rev Sci Instrum 59:1405–1408

Goto T, Anderson OL (1989) Elastic constants of corundum up to 1825 K. J Geophys Res 94:7588–7602

Hearmon RFS (1956) The elastic constants of anisotropic materials II. Adv Phys 5:323–382

Kammer EW, Pardue TE, Frissel HF (1948) A determination of the elastic constants for beta-quartz. J Appl Phys 19:265–270

Koga I, Aruga M, Yoshinaka Y (1958) Theory of plane elastic waves in a piezoelectric crystalline medium and determination of elastic and piezoelectric constants of quartz. Phys Rev 109:1467–1473

McSkimin HJ, Andreatch P, Thurston RN (1965) Elastic moduli of quartz versus hydrostatic pressure at 25 and −195.8°C. J Appl Phys 36:1624–1632

Oda H, Suzuki I, Ohno I (1993) Partial derivatives of eigenfrequencies of a rectangular parallelepiped and a sphere of elastically anisotropic solid. J Phys Earth 41:271–289

Ohno I (1976) Free vibration of a rectangular parallelepiped crystal and its application to determination of elastic constants of orthorhombic crystals. J Phys Earth 24:355–379

Ohno I (1990) Rectangular parallelepiped resonance method for piezoelectric crystals and elastic constants of alpha-quartz. Phys Chem Minerals 17:371–378

Ohno I (1994) Temperature variation of elastic properties of α-quartz up to the α-β transition. J Phys Earth 43:157–169

Ohno I, Yamamoto S, Anderson OL (1986) Determination of elastic constants of trigonal crystals by the rectangular parallelepiped resonance method. J Phys Chem Solids 47:1103–1108

Scott JF (1972) Soft-mode spectroscopy: experimental study of structural phase change. Rev Mod Phys 46:83–127

Zubov VG, Firsova MM (1962) Elastic properties of quartz near the α-β transition. Soviet Phys Cryst 7:374–376